Experimental investigation of the Nb-Ni phase diagram

HAILIN CHEN, YONG DU*, HONGHUI XU, YONG LIU
State Key Laboratory of Powder Metallurgy, Central South University, Changsha, Hunan 410083, Republic of China
E-mail: yong-du@mail.csu.edu.cn

J. C. SCHUSTER
Institut für Physikalische Chemie, Universität Wien, Währingerstrasse 42, A-1090 Wien, Austria

Published online: 16 September 2005

The Nb-Ni system is an important sub-binary system in multi-component Ni-based superalloys which have properties at high temperatures. These properties result mainly from the precipitation of the γ' phase ($L1_2$) based on Ni_3Al or γ'' based on $NbNi_3$ [1]. Many technologically important phases in the multi-component Ni-based alloys contain significant amount of Nb [2]. This binary system is also one of the earliest systems in which an amorphous phase can be produced by mechanical alloying (MA) method [3]. MA method avoids the problems associated with high cooling rate, which places a severe restriction on the synthesis of metallic glass by various quenching techniques. In order to establish the stable phase equilibria and to interpret the relative stabilities of metastable phase equilibria in multi-component Ni-based superalloys, knowledge of the phase diagram and thermodynamic properties in the Nb-Ni binary system needs to be known accurately.

The Nb-Ni system has been assessed by Nash and Nash [4] and modeled by Bolcavage and Kattner [5]. All the literature data reviewed by them [4, 5] together with the data later published are reproduced in Fig. 1. As shown in this figure, the liquidus from Ni to about 50 at.% Nb and the solubility of Ni in Nb are well established experimentally.

The liquidus and solidus in the Ni-rich side were determined by Grube *et al*. [6] and Duerden and Hume-Rothery [7] using the heating curves of thermal analysis, which avoids problems of undercooling. The liquidus lines associated with $NbNi_3$ and μ (Nb_7Ni_6) phases were determined by several groups of investigators using thermal analysis [7–9] and a combination of chemical analysis and thermal analysis [10]. The liquidus from Duerden and Hume-Rothery [7] was preferable since (I) high purity starting materials were used, (II) the experimental procedure was well described, and (III) the melting temperatures for pure Ni and $NbNi_3$ are consistent with the generally accepted ones.

However, there are some uncertainties on the other phase boundaries. The solubility of Nb in Ni was measured by several groups of investigators using different methods, X-ray diffraction (XRD) [6–8, 11, 12], electron probe microanalysis (EPMA) of the diffusion couples [13–16], and metallography [17]. The reported experimental data show noticeable discrepancies and two alternative interpretations for the solubility of Nb in Ni were presented in the assessment due to Nash and Nash [4]. Either the solubility exhibits a rapid decrease from the eutectic temperature (1282 °C) to about 1000 °C [6, 7], or it decreases gradually down to 800 °C [8, 17].

The liquidus in the Nb-rich side was measured by Duerden and Hume-Rothery [7] using optical pyrometry method and Wicker *et al*. [16] employing both chemical analysis and thermal analysis. The liquidus line provided by the former is higher by about 200 °C than that from the latter.

Several groups of authors contributed to the measurement of the homogeneity ranges for $NbNi_3$ [7, 13–15] and μ [7, 8, 13–15, 18] as well as the (Nb) solvus [7, 8, 13–15] using different experimental methods, XRD and metallography [7, 8], EPMA of the diffusion couples [13–15] and EPMA of alloys [18]. There is no general agreement among the published data.

Quist *et al*. [19] and Wekken *et al*. [20, 21] suggested the existence of the $NbNi_8$ phase and found that its nucleation and growth under the critical temperature require large concentration of excess vacancies, produced either by rapid quenching or charged-particle irradiation. It is of interest to verify whether $NbNi_8$ phase is really a stable one.

In order to refine the Nb-Ni phase diagram presented by Nash and Nash [4], ten decisive alloys in the composition range of 5 to 65 at.% Nb were arc-melt under purified argon atmosphere, with 99.99% purity Ni and 99.99% purity Nb (both from Johnson Matthey Company, MA 01835, USA). The compositions of the samples were listed in Table I. No chemical analysis for these alloys was performed since the weight losses during arc-melting were generally less than 0.1 mass %. Each as-cast sample was divided into four pieces. One piece in as-cast state was used for metallographic inspection. The other three pieces were encapsulated in quartz tubes under a vacuum of 10^{-3} bar and then annealed in a high-temperature diffusion furnace (L-45-1-135, Qingdao, China) at different

* Author to whom all correspondence should be addressed.

0022-2461
DOI: 10.1007/s10853-005-4553-4

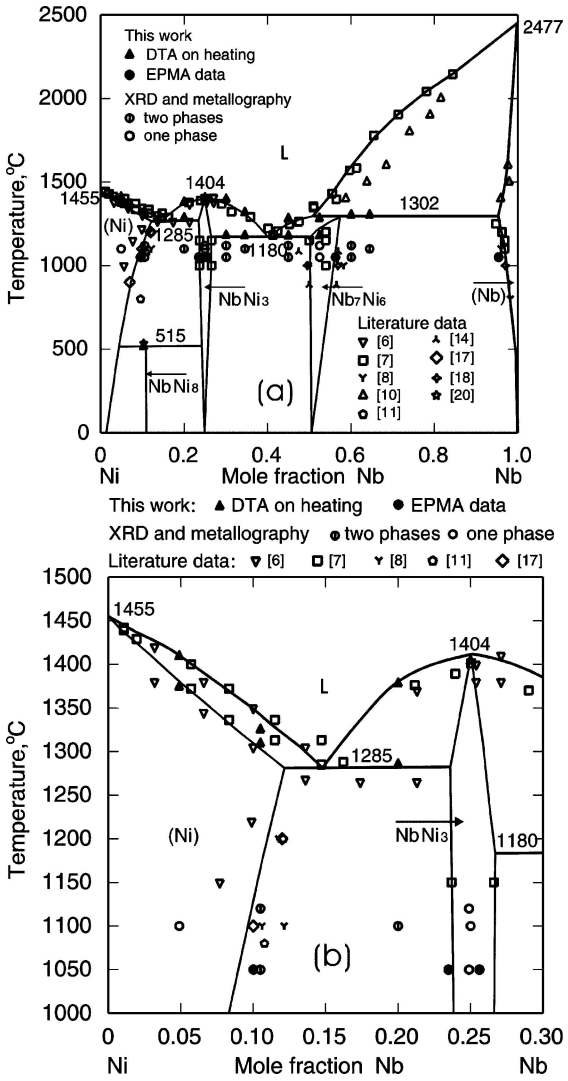

Figure 1 Assessed Nb-Ni phase diagram according to the present work and the literature data, (a) in the whole composition range and (b) from pure Ni to 30 at.% Nb in the temperature range of 1000 °C to 1500 °C.

temperatures for extended periods of time: 1100 °C for 143 hr, 1050 °C for 336 hr, and 1000 °C for 209 hr. The water-quenched samples were analyzed by means of XRD, differential thermal analysis (DTA), and EPMA techniques, supplemented by optical microscopy. The phase identification was made by means of XRD (Rigaku D/max 2550VB, Japan) using Cu Kα_1 radiation with Si as an internal standard. The microstructure observation was performed with optical microscopy (Leica DMLP, Wetzlar, Germany).

A high-temperature DTA apparatus (DTA 701L, Bähr Thermoanalyse GmbH, Germany) was used to measure phase transition temperatures. Solid pieces with weights of about 50 mg were taken from the samples annealed at 1000 °C for 209 hr. The measurement was carried out between room temperature and 1500 °C with a heating and cooling rate of 5 K/min in argon atmosphere. The temperature was measured with Pt-Pt/Rh thermocouples and calibrated to the melting temperatures of Al (660.32 °C), Au (1064.18 °C) and Si (1413.85 °C). The phase transition temperatures were taken from heating curves because supercooling phenomenon usually accompanies solidification and reactions between samples and Al_2O_3 crucible material could not be completely excluded. The accuracy of the temperature measurement was estimated to be ±2 °C.

TABLE I Summary of the phases for the Nb-Ni alloys annealed at 1000 °C for 209 hr, and phase transition temperatures measured by DTA

No.	at.% Nb	Phase[a]	Transition temperature (°C)[b]
1	5	(Ni)	1374, 1409
2	10.5	(Ni)	1309, 1325
3	20	(Ni) + Ni_3Nb	1285, 1378
4	25	Ni_3Nb	1404
5	30	$Ni_3Nb + \mu$	1181, 1396
6	34.5	$Ni_3Nb + \mu$	1180, 1317
7	45	$Ni_3Nb + \mu$	1178, 1280
8	52.5	μ	1180, 1282
9	60	μ + (Nb)	1302
10	64.5	μ + (Nb)	1303

[a]The phases are identified by means of XRD and metallography.
[b]The transition temperatures were obtained from the heating curves with a heating rate of 5 K/min.

In order to measure the temperature associated with the peritectoid reaction (Ni) + $NbNi_3$ = $NbNi_8$ accurately, the arc-melted alloy $Nb_{0.1}Ni_{0.9}$ was annealed at 500 °C for 45 days, water-quenched, and then subjected to DSC (DSC 404C, NETZSCH, Selb/Bavaria, Germany) measurement up to 700 °C under a flow of 99.998% purity Ar with a heating rate of 5 K/min. The sample was wrapped with Ta foil before put into Cu pan in order to avoid the reaction between the samples and Cu pans. Another Ta foil with the same weight as that in the sample holder was inserted into Cu reference holder. The temperature in DSC measurement was calibrated to pure elements In, Pb, and Zn.

Table I summarizes the phases identified by XRD and optical microscopy along with the phase transition temperatures resulting from DTA measurements. The eutectic reactions (L = (Ni) + $NbNi_3$ and L = $NbNi_3$ + μ), peritectic reaction (L + (Nb) = μ) and the congruent melting feature of $NbNi_3$ are confirmed in the present work by the use of XRD and optical microscope. Table II lists the invariant reaction temperatures from various sources including the present measurement.

In these excellently reproducible measurements, the general features of the previously established Nb-Ni phase diagram are confirmed. However, the quantitative data need to be revised and an amendment of the phase diagram published in a recent paper [4] is necessary.

The DTA measurement of the alloy $Nb_{0.2}Ni_{0.8}$ shows that the eutectic reaction L=(Ni)+$NbNi_3$ occurs at 1285 ± 2 °C. This temperature corroborates the value of 1285 °C from Svechnikov *et al.* [8] and the average temperature of 1282 °C resulting from the measurement of four samples [7]. Compared with the above temperatures, the values of 1270 °C form Pogodin and Selikmann [17] and 1265 °C due to Grube *et al.* [6] appear relatively low.

For the alloy $Nb_{0.25}Ni_{0.75}$ annealed at 1000 °C for 209 hr, the only DTA signal was observed at 1404 ± 2 °C. Optical microscopy examinations of the as-cast

TABLE II Summary of the measured invariant reaction temperatures (°C) in the Nb-Ni system

Reaction	This work	[7]	[10]	[15]	[16]	[17]	[20]
$L \leftrightarrow NbNi_3$	1404 ± 2	1402	1430	1403		1400	
$L + (Nb) \leftrightarrow \mu$	1302 ± 2	1295	1320		1290		
$L \leftrightarrow (Ni) + Nb\ Ni_3$	1285 ± 2	1282	1285	1270			
$L \leftrightarrow Nb\ Ni_3 + \mu$	1180 ± 2	1175	1170	1175	1175		
$(Ni) + Nb\ Ni_3 \leftrightarrow \mu$	515 ± 2						≈535

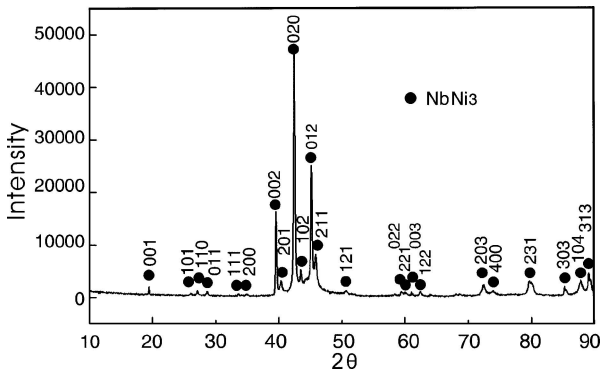

Figure 2 X-ray diffraction pattern for the sample $Ni_{0.75}Nb_{0.25}$ annealed at 1000 °C for 209 hr.

and annealed states reveal the existence of $NbNi_3$ single phase, which is confirmed by XRD measurement, as shown in Fig. 2. In Table III, the presently calculated lattice parameters for $NbNi_3$ phase were compared with those in Villars and Calvert's handbook [22], showing a reasonable agreement. Thus, it is concluded that the measured congruent melting temperature for $NbNi_3$ is 1404 ± 2 °C, which is in nearly perfect agreement with the value of 1402 °C from Duerden and Hume-Rothery [7]. The present value also agrees very well with the temperature of 1400 °C from Kornilov and Pylaeva [9], and 1403 °C from Pogodin and Selikmann [17]. Only compared with the data of Svechnikov *et al.* [8], there is a discrepancy. This discrepancy could be due to the imperfect temperature calibration in the experiment of Svechnikov *et al.* [8]. Their calibration [8] for temperatures less than 1500 °C was done with pure Fe assuming the transformation γ(fcc_A1(Fe))↔δ(bcc_A2(Fe)) to occur at 1440 °C rather than the generally accepted value of 1394 °C, as pointed out by Kocherzhinsky [23]. This might have played a role in causing the discrepancies in the Nb-Ni system too.

The DTA measurements on three alloys $Nb_{0.3}Ni_{0.7}$, $Nb_{0.35}Ni_{0.65}$ and $Nb_{0.45}Ni_{0.55}$ result in the temperature of 1180±2 °C for the eutectic reaction L=$NbNi_3$+μ. This temperature is slightly higher than the literature value of 1175 °C from three groups of investigators [7, 10, 17].

DTA measurement for the alloys $Nb_{0.6}Ni_{0.4}$ and $Nb_{0.65}Ni_{0.35}$ up to 1500 °C was performed. Only one DTA signal was observed at 1302±2 °C for both alloys. This temperature is assigned to be the reaction temperature for L+(Nb)=μ. This value is somewhat higher than 1290 °C from Wicker *et al.* [10] and 1295 °C from Duerden and Hume-Rothery [7]. However, Svechnikov *et al.* [8] reported an even higher value of 1320 °C. This discrepancy could be also due to their improper calibration in the experiment of Svechnikov *et al.* [8]. In the literature, there are two measurements on the Nb-rich liquidus. The liquidus temperature published by Duerden and Hume-Rothery [7] is much higher than that by Wicker *et al.* [10], as shown in Fig. 1. Had the liquidus established by Wicker *et al.* [10] been accurate, the liquidus temperature for the alloy $Nb_{0.6}Ni_{0.4}$ should be below 1500 °C. The present DTA measurement shows that this is not the case. Consequently, the Nb-rich liquidus provided by Duerden and Hume-Rothery [7] is consistent with the present measurement.

The XRD examination on the alloy $Nb_{0.1}Ni_{0.9}$ annealed at 500 °C for 45 days shows that the $NbNi_8$ single phase is present, as seen from Fig. 3. As shown in Table III, the lattice parameter calculated for $NbNi_8$ phase agrees well with that reported by Ardell [24]. The Bravais lattice for $NbNi_8$ phase is body centered tetragonal (b.c.t), while its crystallography can also be conveniently described by the larger face centered tetragonal (f.c.t) unit cell and the constant a_0' in the f.c.t cell equals the constant a_0 in the b.c.t cell multiples by $\sqrt{2}$ [24]. Wekken *et al.* [20] reported the lattice parameter in terms of the f.c.t unit cell. This value is comparable with that in this work after a corresponding conversion, as shown in Table III. The DSC measurement on this annealed alloy shows a thermal effect at 515 °C, which is assigned to be the temperature for the peritectoid reaction $(Ni) + NbNi_3 = NbNi_8$. This temperature is lower by 20 °C than the approximate temperature from Wekken *et al.* [20], who estimated the reaction

TABLE III Summary of the measured lattice parameters (nm) for the $NbNi_3$ and $NbNi_8$ phases

Phases	Space Group	Pearson Symbol	*a*	*b*	*c*	Reference
$NbNi_3$	Pmmn	*t*I8	0.5021	0.4240	0.4627	This work[a]
			0.5116	0.4259	0.4565	
$NbNi_8$	I4/mmm	*t*I18	0.7615	0.7615	0.3589	This work[b]
			0.7612	0.7612	0.3593	[24]
			0.7638	0.7638	0.3600	[20]

[a]The alloy $Nb_{0.25}Ni_{0.75}$ annealed at 1000 °C for 209 hr was used for XRD measurement.
[b]The alloy $Nb_{0.10}Ni_{0.90}$ annealed at 500 °C for 45 days was used for XRD measurement.

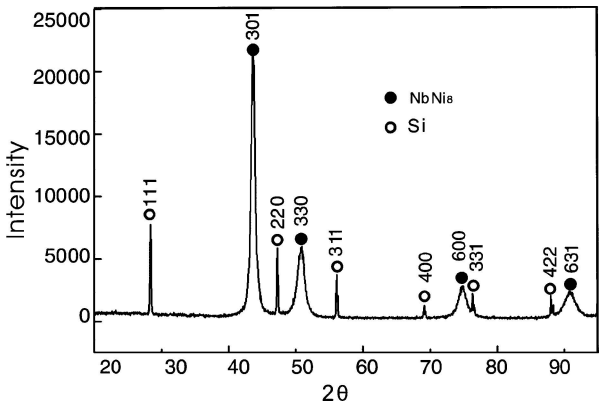

Figure 3 X-ray diffraction pattern for the sample $Ni_{0.9}Nb_{0.1}$ annealed at 500 °C for 45 days with Si as an internal standard.

temperature by means of the electrical resistivity measurement.

To get some insight into the homogeneity ranges for $NbNi_3$ and μ as well as the mutual solid solubility between Nb and Ni, EPMA (JXA-8800R, JEOL, Japan) measurement on the alloys annealed at 1050 °C for 209 hr was performed. Pure Nb and Ni, which were subjected to the same treatment as that employed for the alloys, are used as standards. Conventional matrix correction, which deals with the deviation from linearity by including the effects of atomic number (Z), absorption (A) and fluorescence (F), was employed to calculate the compositions from the measured X-ray intensities with an accelerating voltage of 20 kV and a beam current of 20 nA. The obtained experimental data are shown in Fig. 1 along with the literature data.

The starting materials with high purity are used in the present work and the experimental results from several approaches are consistant with each other. This implies that the present experimental results are reliable. Based on the critical review of experimental phase diagram data, supplemented by new measurement, the revised Nb-Ni phase diagram is presented in Fig. 1. The presently revised Nb-Ni phase diagram is also shown in Fig. 4 for easy perception without the data points and in the practical Celsius scale. This phase diagram is expected to substitute for the currently accepted version [4, 5].

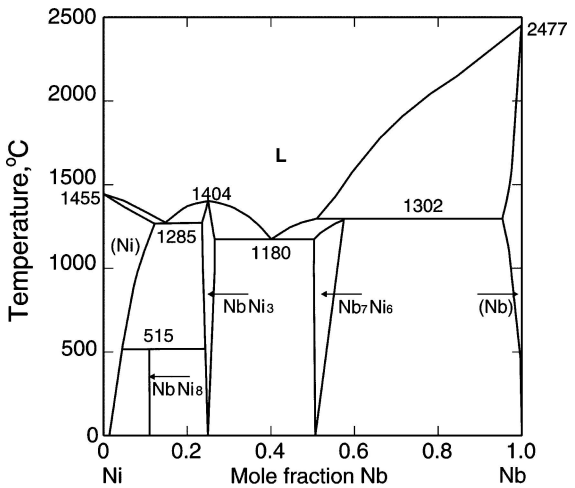

Figure 4 Assessed Nb-Ni phase diagram according to the present work.

Acknowledgments

This research work is supported by National Outstanding Youth Science Foundation of China (Grant No. 50425103) and National Advanced Materials Committee of China (Grant No. 2003AA302520). Y. Du gratefully acknowledges the Furong Chair Professorship program released by Hunan province of P.R. China for financial support. The donation of Leica DMLP microscope from Alexander von Humboldt Foundation is also greatly appreciated.

References

1. N. DUPIN and I. ANSARA, *J. Phase Equilibria* **14** (1993) 451.
2. K. M. CHANG, H. J. LAI and J. Y. HWANG, in "Superalloys 718, 625, 706 and Various Derivatives", Proc. Int. Symp., 3rd, 1994, edited by E.A. Loria (Miner. Met. Mater. Soc., Warrendale PA, 1994) p. 683.
3. P. Y. LEE and C. C. KOCH, *J. Non-Cryst. Solids* **94** (1987) 88.
4. P. NASH and A. NASH, *Bull. Alloy Phase Diagrams* **7** (1986) 124.
5. A. BOLCAVAGE and U. R. KATTNER, *J. Phase Equilibria* **17** (1996) 92.
6. G. GRUBE, O. KUBASCHEWSKI and K. ZWIAUER, *Z. Elektr Chem.* **45** (1939) 881.
7. I. J. DUERDEN and W. HUME-ROTHERY, *J. Less-Common Met.* **11** (1966) 381.
8. V. N. SVECHNIKOV, V. M. PAN and V. G. KOROBEINIKOVA, *Sb. Nauchni. Metallofiz., Akad. Nauk Ukr. SSR* **19** (1964) 196.
9. I. I. KORNILOV and E. N. PYLAEVA, *Izv. Akad. Nauk. SSSR, Met.* **5** (1966) 132.
10. A. WICKER, C. ALLIBERT, J. ORIOLE and E. BONNIER, *C.R. Acad. Sci. C* **271** (1970) 273.
11. L. N. GUSEVA, R. S. MINTS and Y. S. MALKOV, *Russ. Metall.* **5** (1969) 120.
12. D. S. DUVALL and M. J. DONACHIE, *J. Inst. Met.* **98** (1970) 182.
13. W. SPRENGEL, M. DENKINGER and H. MEHRER, *Intermetallics* **2** (1994) 137.
14. Y. MURAMATSU, *Trans. Nat. Res. Inst. Met.* **17** (1975) 21.
15. Y. MURAMATSU, F. ROUX and A. VIGNES, *Trans Jpn. Inst. Met.* **16** (1975) 61.
16. H. T. BERTORELLO, R.W. HERTZBERG, W. MILLS, R.W. KRAFT and M. NOTIS, *Acta Metall.* **24** (1976) 271.
17. S. A. POGODIN and A. N. SELIKMANN, *C.R. Dokl. Akad. Sci. URSS* **31** (1941) 895.
18. J. M. JOUBERT and Y. FEUTELAIS, *Calphad* **26** (2002) 427.
19. W. E. QUIST, C. J. WEKKEN, R. TAGGART and D.H. POLONIS, *Trans. Met. Soc. AIME* **245** (1969) 345.
20. C. J. WEKKEN, R. TAGGART and D. H. POLONIS, *J. Met. Sci.* **5** (1971) 219.
21. C. J. WEKKEN, J. M. LARSON, R. TAGGART and D. H. POLONIS, *J. Appl. Phys.* **43** (1972) 4522.
22. P. VILLARS and L. D. CALVERT, in "Pearson's Handbook of Crystallographic Data for Intermetallic Phases, American Society for Metals" (International, Materials Park, OH, 1985) p. 2814.
23. Y. A. KOCHERZHINSKY, in "Thermal Analysis", Proc. Third ICTA Davos (Birkhäuser Verlag, Basel, 1971) p. 549.
24. A. J. ARDELL, in "Metallic Alloys: Experimental and Theoretical Perspectives" (Kluwer Academic Publishers, Dordrecht, 1994) p. 93.

Received 18 February 2004
and accepted 13 April 2005